Controlled destruction of chaos in the multistable regime

B. K. Goswami*
Laser and Plasma Technology Division, Bhabha Atomic Research Centre, Mumbai 400085, India
(Received 26 December 2006; published 31 July 2007)

Autonomous nonlinear systems commonly exhibit simultaneous coexistence, in the phase space, of chaos and stable steady states, created by subcritical Hopf bifurcation. We show that such chaotic instability can be destroyed by small-amplitude modulation of any system parameters. The chaotic attractor undergoes boundary crisis due to a modulation-induced collision with an unstable periodic orbit (UPO). Such a boundary crisis exhibits a new resonance that we refer to as "crisis resonance" in the control parameter space. Crisis resonance implies that crisis occurs at minimum modulation depth due to resonant evolutions of the UPOs and the chaotic attractor. Crisis resonance occurs close to some critical frequency (we refer to it as "crisis resonance frequency") or its multiples. The UPO frequency is a good estimate of the crisis resonance frequency. The small-amplitude parameter modulation destroys chaos in the presence of noise as well. These features are observed theoretically with the paradigm of autonomous systems, namely, Lorenz equations of thermal hydraulics and are in excellent agreement with the experimental results, obtained with an analog circuit of Lorenz equations.

DOI: 10.1103/PhysRevE.76.016219 PACS number(s): 05.45.−a, 44.25.+f, 47.52.+j, 42.65.Pc

In the recent past, controls in the form of small perturbations have been shown to create fascinating effects in the dynamics of nonlinear systems; in particular, techniques such as (i) controlling chaos (using OGY concepts [1] or the proportional feedback method [2]) and (ii) tracking the unstable steady states [3]. These techniques are in general model independent and have found wide applicability in varied branches of science including human heart or brain related nonlinear sciences, fluid dynamics, electronics, chemical reactions, lasers, etc. When a system is chaotic and there is no coexisting stable steady (or periodic) attractor, one of the major objectives of control of chaos is to get rid of chaotic irregularity by stabilizing the dynamics at an unstable stationary (periodic) state (embedded inside the chaotic orbit) with the help of such small control perturbations. A detailed review in this direction and a comprehensive list of references may be seen in Boccaletti *et al.* [4]. Unless the system parameter values are grossly shifted out of the chaotic regime, one hurdle still remains in such occasions: The system goes back to the chaotic state as soon as the control is switched off. However, the scenario could be grossly different when the chaotic attractor coexists in the phase space with some stable steady states (or periodic) states (multistability) and the major objective is to move the system out of the chaotic state and bring in any of those stable steady (periodic) states. Under such circumstances, it would be preferable to devise a deterministic control mechanism to destroy the chaotic state, so that the system, as a consequence, settles into a neighboring stable state and remains there even if the control is switched off. In this paper, we will demonstrate such a control mechanism for autonomous nonlinear systems that commonly exhibit multistability in the form of simultaneous coexistence in the phase space of chaotic instability and steady states, created by subcritical Hopf bifurcation. To name a few such systems, (i) optically injected NMR [5], CO_2 [6,7], and semiconductor lasers [8,9], (ii) far infrared (FIR) lasers [10,11], (iii) thermal hydraulics in two-phase natural circulation fluid dynamics [12–14], (iv) nonlinear electronic circuits [15,16], and (v) plasma[17].

The objective of this paper is to explore the effect of small-amplitude periodic modulation of system parameters on such chaotic instability. These investigations are motivated not only from the viewpoint of basic research but keeping in mind its wide applicability. In particular, we would be interested to know whether such modulation may lead to the destruction of chaotic instability so that the system could regularly remain at steady states even in the multistable operating regime. We believe such a concept may then be useful to many autonomous systems (applications) that are designed to remain at steady states and the extension of the operating regimes in the multistable regions are beneficial. We consider the paradigm of autonomous nonlinear systems, namely, Lorenz equations of thermal hydraulics [18] and demonstrate theoretically the modulation-induced boundary crisis of the Lorenz chaotic attractor, and validate experimentally with its analog circuit. Lorenz equations are described by

$$\dot{X} = -\sigma(X - Y),$$

$$\dot{Y} = rX - Y - XZ,$$

$$\dot{Z} = XY - bZ. \tag{1}$$

Figures 1 and 2 show some of our numerical results of Eqs. (1). In plot (a) of Fig. 1 we show the bifurcation diagram with r as the control parameter ($\sigma=10$, $b=1.2$). The trivial steady state ($X=Y=Z=0$), denoted by "O" (the horizontal solid line), undergoes pitchfork bifurcation at the point P and two stable nontrivial steady states, denoted by S_+ and S_- are created. Each nontrivial steady state undergoes subcritical Hopf bifurcation [loss of stability due to collision with a coexisting unstable periodic orbit (UPO)] at $r=r_H$ (at the points H). The curve above the line represents the minimum-X points of U_+ UPOs (around S_+) at various values

*Electronic address: binoy@barc.gov.in

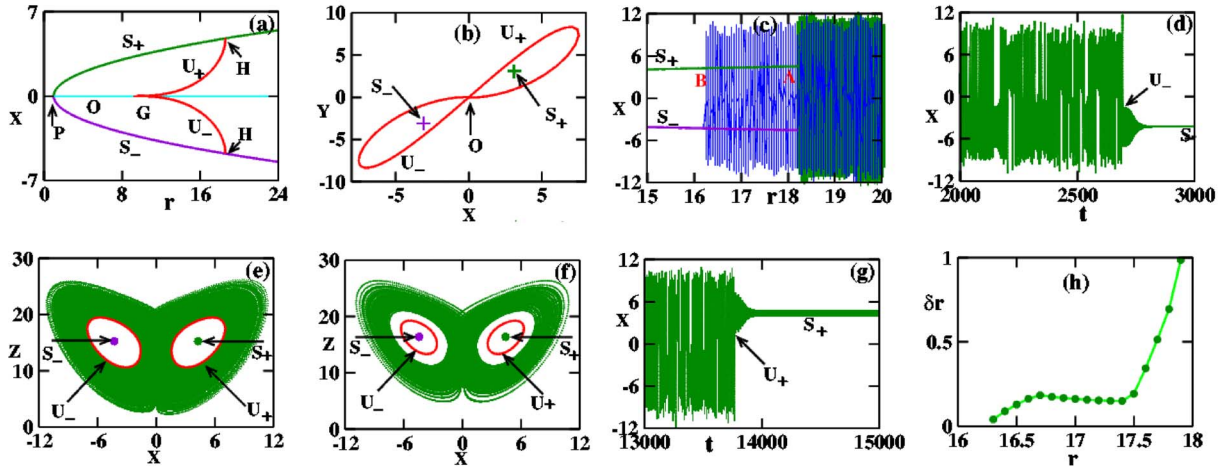

FIG. 1. (Color online) Controlled destruction of Lorenz chaos. $\sigma=10$, $b=1.2$. These values remain unchanged in this figure. (a) The bifurcation diagram with r as the control parameter. The steady state branch ($X=Y=Z=0$), shown by the horizontal solid line, undergoes pitchfork bifurcation at the point P and two stable nontrivial steady states S_+ and S_- are created. Each of these nontrivial steady states undergoes subcritical Hopf bifurcation at the point H. The curve, above the trivial steady-state branch, represents the minimum-X values of the UPO U_+ at various values of r. Similarly, the curve, below the trivial steady-state branch, denotes the maximum-X values of the UPO U_-, respectively. At the point G, both the UPOs become biasymptotic to the saddle steady state, creating a figure-of-eight homoclinic orbit (gluing bifurcation). (b) The phase portrait of the biasymptotic homoclinic orbit around the saddle state (O) and the stable nontrivial steady states (denoted by plus symbols). (c) Bifurcation diagram with r as the control parameter. In the case of increasing r, the steady states (solid lines) undergo subcritical Hopf bifurcations at $r=r_H$ (denoted by the point "A"). The system jumps to the chaotic state (the superposition of shaded regions [darker]) for $r>r_H$. On the contrary, when r is reduced from such a high value, chaos coexists in the phase space with the steady states until there is another jump back to any of these steady states at $r=r_c$ (denoted by the point "B"). (d) The temporal destruction of the chaotic attractor at $r=16.18$ due to the collision with the UPO U_- and the subsequent transition to the steady state S_-. (e) The phase portraits of the Lorenz chaos and the UPOs at $r=16.2488$. The circles in the middle of the UPOs denote the stable steady states. The UPOs lie in the boundary of the chaotic attractor that results in the crisis. (f) The phase portraits of the chaotic attractor, UPOs, and the steady states at $r=17.0$. (g) The temporal destruction of Lorenz chaos due to the introduction of periodic modulation over r with amplitude $\delta r=0.006$ and frequency $\nu=0.8$ at $r=17.0$. The crisis occurs due to the collision of the chaotic transients with the UPO U_+. Past the crisis the system jumps to the controlled S_+ state. (h) The crisis threshold amplitude δr versus r; $\nu=0.8$.

of r. The curve below the line denotes the maximum-X points of U_-, UPOs (around S_-), respectively. As one reduces r from r_H, these UPOs grow bigger in size in the phase space. At $r=r_G\cong 9.0$ (denoted by G), the UPOs become biasymptotic to the trivial saddle (O), creating homoclinic orbit (gluing bifurcation) [19–22]. Plot (b) shows the homoclinic orbit around the trivial saddle (O), created by the composure of U_+, U_- and the saddle O. The stable nontrivial steady state S_+ (plus symbol) lies inside U_+ and S_- (plus symbol) within U_-. Plot (c) shows the overall bifurcation diagram with r as the control parameter; $\sigma=10$, $b=1.2$. In the case of forward sweep (increasing r), the steady states S_+ (solid lines) and S_- (solid line) undergo subcritical Hopf bifurcations at $r_H\cong 18.25$ (denoted by "A"). Lorenz chaos (the superposition of the shaded regions) is observed for $r>r_H$. On the contrary, when r is reduced from such a high value, the chaotic attractor (shaded region) coexists in the phase space with the steady states until there is another jump back to any of these steady states at $r=r_c\cong 16.25$ (denoted by "B"). Thus the multistable interval (denoted by BA) is between $16.25\leq r\leq 18.25$. The jump at $r=r_c$ occurs because the chaotic attractor collides with any UPOs leading to boundary crisis. Plot (d) shows such a crisis due to the collision with the U_+ UPO at $r\cong r_c$ and subsequent transition to the steady state S_+. The boundary crisis is illustrated more through phase portraits of Lorenz chaos and the UPOs in plot (e). U_+ and U_- lie in the closure of the chaotic attractor. This leads to the crisis and after chaotic transients, the iterations converge to either of the steady states S_+ (circular symbol) or S_- (circular symbols).

We demonstrate now the controlled destruction of Lorenz chaos within the multistable region $r_c<r<r_H$ by a small-amplitude sinusoidal modulation over any system parameters. As a typical example, first we consider the modulation over r in the form of $r[1+\delta\cos(2\pi\nu t)]$. By "small" amplitude (say δr), we imply that no qualitative change would occur in the dynamics if r is changed by δr without any modulation. In other words, if the unmodulated system is originally chaotic, it will remain chaotic even if r is changed by δr. We first fix the operating value of $r=17.0$ as an example, and show the phase portraits of the chaotic attractor, UPOs, and the stable steady states in plot (f). Next we introduce the modulation over r with frequency $\nu=0.8$. As the modulation depth δ is increased beyond 0.006, the chaotic attractor undergoes boundary crisis. Plot (g) illustrates the temporal destruction of the chaotic attractor due to collision with the U_+ UPO and subsequent transition to the controlled steady state S_+. The system remains at the same steady state even when the control is switched off. The threshold (minimum) modulation amplitude (δr) to create such a crisis depends on the remaining system parameters. For instance, in plot (g) we show the dependence of the threshold amplitude

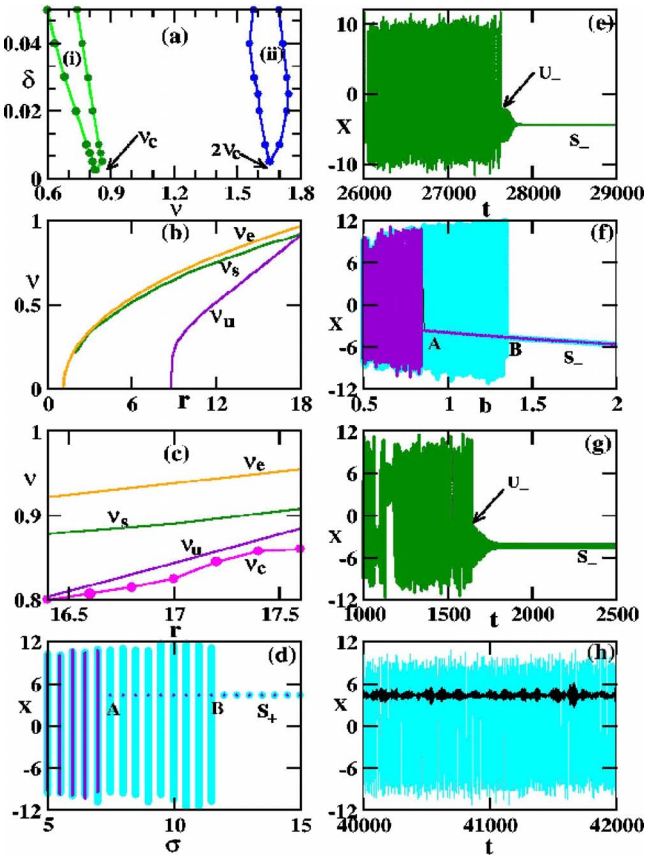

FIG. 2. (Color online) (a) Chaos destruction boundaries in $(\delta-\nu)$ space; $r=17$, $b=1.2$, $\sigma=10$. The crisis resonance frequency $\nu_c=0.825$. (b) Steady-state resonance frequency ν_s, steady-state eigenfrequency ν_e, and the UPO frequency ν_u curve). (c) The curves of plot (b) are enlarged in the vicinity of Hopf bifurcation. In addition, the crisis resonance frequency ν_c is shown by the curve. Notice that ν_c is in the close neighborhood of ν_u. (d) Bifurcation diagram with σ as the control parameter; $r=17$, $b=1.2$. (e) Controlled crisis due to collision with U_- UPO and the subsequent transition to the controlled S_- state; $\sigma=10$, $\nu=1.7$, $\delta=0.1$. (f) Bifurcation diagram with b as the control parameter; $r=17$, $\sigma=10$. (g) Controlled destruction of Lorenz chaos due to a collision with U_- and the subsequent transition to the controlled S_- state because of b modulation: $b=1.2$, $\nu=0.82$, $\delta=0.02$. (h) Controlled destruction of Lorenz chaos in the presence of noise. The time series represents noisy Lorenz chaos; $r=17$, $b=1.2$, $\sigma=10$, $\rho=1.0$. As the modulation is introduced ($\nu=0.8$, $\delta=0.01$), the chaotic attractor is destroyed and the system jumps to the noisy steady state under control time series.

δr versus r at the same frequency. One may notice that the threshold amplitude is relatively large near the Hopf bifurcation region ($r\cong r_H$). This is expected because the phase-space separation between the chaotic attractor and the UPOs is the largest near $r=r_H$. Therefore, to induce crisis, the required modulation amplitude could be relatively large. By a similar argument one can explain the smallest threshold amplitude near the crisis point ($r=r_c$) where the UPOs are in the close proximity of the chaotic attractor. Overall, we may also notice that the parameter modulation technique is very effective to create the boundary crisis even at small modulation amplitude. For instance, consider the operating point at $r=17.5$. Plot (c) suggests that r should be decreased by $r-r_c=1.25$ to create the crisis without modulation. However, if we introduce the parameter modulation, the same may be performed by modulation amplitude $\delta r\cong 0.2$ [see plot (h)]. In fact, along a broad range of the multistable region, chaos can be destroyed in a similar manner where the threshold modulation amplitude would be much smaller than the gross change of r, required for destruction of unmodulated Lorenz chaos. Moreover, in the case of parameter modulation, the time required to destroy the transient chaos could be shortened by operating at a little higher than the threshold modulation depth. This is because the transient chaos decays very fast if δ is increased even slightly beyond its threshold.

Plot (a) in Fig. 2 shows two threshold destruction boundaries [(i) and (ii)] in $(\delta-\nu)$ space for $r=17$, $b=1.2$, $\sigma=10$. The chaotic attractor is destroyed if the modulation parameters lie within any of these boundaries. Significantly, the plot also shows that the threshold amplitude is minimal when the modulation frequency is equal to some critical frequency (we denote by $\nu_c=0.825$) or its double ($2\nu_c$). This is a typical feature of some resonance phenomenon that we refer to as "crisis resonance." (By "crisis resonance" we imply that crisis occurs at minimum modulation amplitude due to resonant evolutions of the UPOs and the chaotic attractor.) Our analyses suggest that the first crisis resonance occurs around $\nu_c=0.825$ and the second resonance around $2\nu_c$. To explore more about the crisis resonance, we analyze a few more characteristic frequencies of the Lorenz model, namely, UPO frequency (ν_u), steady-state eigenfrequency (ν_e), and steady-state resonance frequency (ν_s). (The steady-state eigenfrequency ν_e is defined as the imaginary part of the complex pair of eigenvalues, divided by 2π, of the Jacobian one obtains after linear stability analyses around the steady states.) For fixed $\sigma=10$ and $b=1.2$ values, we compute ν_e for various values of r, shown by the curve. The UPO frequency (ν_u) is shown by the curve. (Steady-state resonance frequency, for given values of σ, b, *and* r, is defined as the modulation frequency at which the linear dynamical response to the periodic parameter modulation exhibits a maximal behavior.) To compute ν_s, we fix $\sigma=10$, $b=1.2$, $r=16.5$, and monitor the dynamical response of the Lorenz equations by modulating r with $\nu=0.8$ and very small modulation depth ($\delta=0.0002$). The initial conditions are selected from the basins of steady states. Lorenz model dynamics follows the modulating signal. We sweep the modulation frequency and indeed notice the maximal behavior of the frequency response at $\nu=\nu_s$. We compute ν_s over a broad range of r and it is shown by the curve in plot (b). One notices that ν_s matches closely with the eigenfrequency ν_e in the $r<r_G$ range. This is because there are only two stable steady states and no UPOs, nor any stable chaotic attractor in this parameter regime. Therefore, the resonance is purely determined by the steady states. As r is increased beyond r_G, the deviation between ν_s and ν_e marginally increases. In this region, the resonance is influenced by the presence of UPOs in addition to the steady states. As we approach the Hopf bifurcation region, the UPO size becomes smaller and its effect on the small-signal resonance becomes more prominant. This

may be noted by the fact that ν_s converges to ν_u in the Hopf bifurcation limit.[1] We concentrate now on the multistable region. All the characteristic frequency curves in plot (b) have been shown with better resolution in plot (c). We also show here the crisis resonance frequency ν_c curve. One would notice that ν_u lies close to ν_c while ν_s is larger and ν_e differs most. In other words, the crisis resonance occurs when the modulation frequency is close to the UPO frequency.

So far we demonstrated the effect of periodic modulation over r in destroying the chaotic attractor. The same feature is observed by modulating other parameters as well, namely, σ and b. For instance, plot (d) shows the multistable regime with σ as the control parameter without modulation; $r=17$ and $b=1.2$. The steady state S_+ undergoes subcritical Hopf bifurcation at $\sigma \equiv \sigma_H = 7.0$ (the point A) and Lorenz chaos is observed for $\sigma < \sigma_H$. If we keep increasing σ here on, we observe that the chaotic attractor coexists with the steady states for a large range of σ until the boundary crisis occurs at $\sigma \equiv \sigma_c \cong 11.5$ (at the point B). Thus the multistable interval in the σ axis is denoted by AB. In this multistable regime, we have observed the controlled death of Lorenz chaos by small-amplitude periodic modulation over σ. For instance, plot (e) shows the temporal destruction of Lorenz chaos in the second crisis resonance region ($\sigma=10$, $\nu=1.7$, $\delta=0.1$) due to the collision with the U_- UPO. Similar controlled crises have also been observed with b modulation. Plot (f) shows the bifurcation diagram with b as the control parameter for the unmodulated Lorenz model ($\sigma=10$, $r=17$). The steady state S_- undergoes subcritical Hopf bifurcation at $b \equiv b_H \cong 0.85$ (denoted by the point "A"). For $b < b_H$ Lorenz chaos is observed. As b is increased from b_H, Lorenz chaos coexists with the steady state S_- until the boundary crisis occurs at $b \equiv b_c \cong 1.35$ and the simulations settle down to the S_- steady state for $b > b_c$. Plot (g) shows a typical example of controlled destruction of chaos by b modulation ($b=1.2$, $\delta=0.02$, $\nu=0.82$). In each of the three types of parameter modulations, the crisis resonance occurs when the modulation frequency is close to the UPO frequency. Also, crisis threshold curves exist around such crisis resonance frequency or its multiples. Therefore, it is apparent that a small-amplitude modulation over any parameter is effective in creating global changes (such as the death of the chaotic attractor) if the modulation frequency is chosen within the resonance regions. Also such a crisis occurs due to UPO-induced resonance. Finally, in plot (h) we demonstrate the applicability of this method in the presence of noise. We introduce to each equation in Eqs. (1) an additive white Gaussian noise of standard deviation ρ and average value zero. The time series shows a typical example of noisy Lorenz chaos for $\sigma=10$, $r=17$, $b=1.2$, $\rho=1.0$. Next we apply control modulation over r ($\nu=0.8$, $\delta=0.01$) to notice the destruction of chaos and the system goes to a noisy steady state, driven by periodic modulation. All these features indicate the versatility of the parameter modulation approach.

[1]For $r \ll r_H$, ν_u grossly differs from ν_s and ν_E, the UPO frequency sharply decreases as we decrease r. At the gluing bifurcation limit ($r=r_G$) the frequency approaches zero.

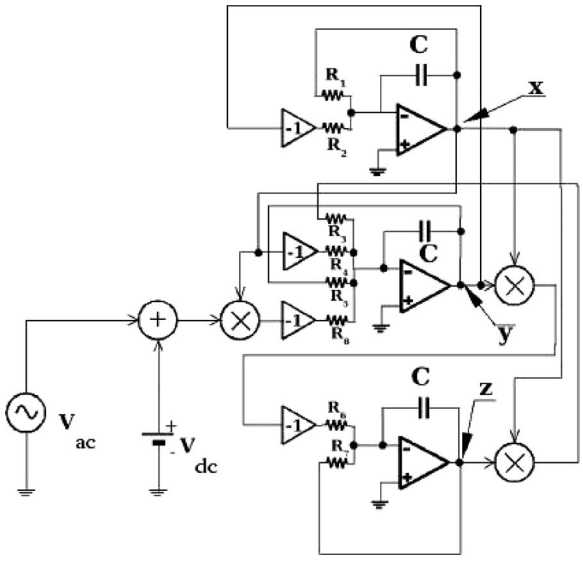

FIG. 3. An analog circuit of Lorenz equations.

These theoretical results are in good agreement with our experimental observations [23] with an analog circuit of Lorenz equations (Fig. 3). The circuit equations are as follows:

$$\dot{X} = -\frac{1}{R_1 C}(X - Y),$$

$$\dot{Y} = -\frac{1}{R_3 C}XZ + \frac{1}{R_4 C}X - \frac{1}{R_5 C}Y + \frac{V_d}{R_8 C}X,$$

$$\dot{Z} = -\frac{1}{R_6 C}XY - \frac{1}{R_7 C}Z. \tag{2}$$

The circuit components are as follows: $R_1=R_2=50$ kΩ, $R_3=R_6=5$ kΩ, $R_4=25$ kΩ, $R_5=100$ kΩ, $R_7=333$ kΩ, $R_8=100$ kΩ, $C=1$ nF. In the schematic diagram of the analog circuit, conventional symbols are used to describe the operational amplifiers, analog multipliers, and inverters. For a generalized experimental setup of Lorenz circuit we have the provision of two voltage sources, represented by V_{dc} and V_{ac}. For the experiments reported here, V_{dc} represents the dc offset voltage while V_{ac} denotes the periodic component. $V_{ac} = \delta |V_{dc}| \cos(2\pi\nu t)$ where the symbol $\|$ implies the absolute magnitude of V_{dc} and δ refers to the control modulation depth. We may note that the parameter σ in the Lorenz equation may be correlated to $\frac{V_d}{R_1 C}$, where $V_d = V_{dc} + V_{ac}$. Similarly, $\frac{1}{R_7 C}$ to b and $\frac{1}{R_4 C} + \frac{V_d}{R_8 C}$ to r. Some experimental results with this circuit are presented in Fig. 4. Plot (a) depicts the generalized bistability with V_{dc} as the control parameter without any modulation ($V_{ac}=0$). The bifurcation diagram with increasing V_{dc} is denoted by the symbols. The circuit remains at the steady state S_+ until $V_{dc}=-1.5$ V (the point "A") and then undergoes subcritical Hopf bifurcation and jumps to chaos where it remains even if we increase V_{dc} further. From such a high value, we then decrease V_{dc} and notice that the circuit remains chaotic until $V_{dc} \cong -2.5$ V (the point B). Thus the bistable region BA is -2.5 V $< V_{dc} < -1.5$ V. These observations are very much similar to the theoretical results in

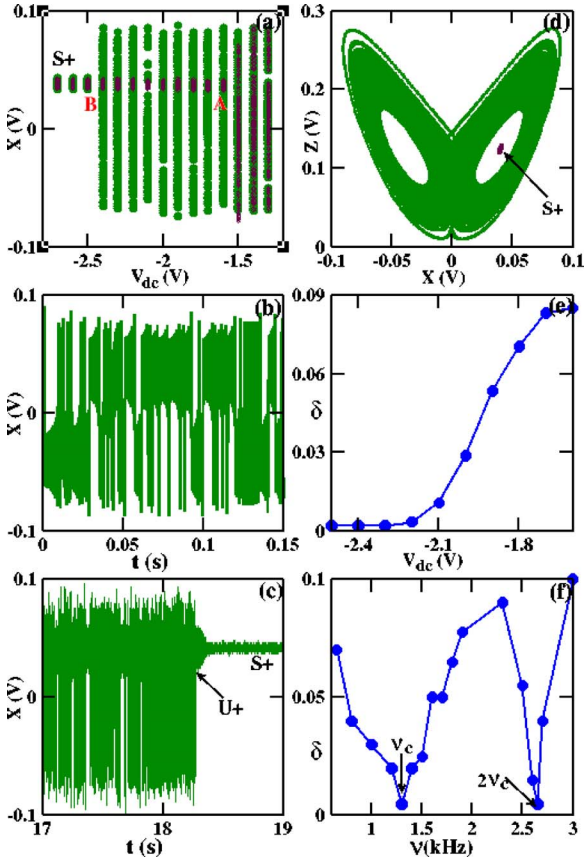

FIG. 4. (Color online) Experimental demonstration of the controlled crisis of Lorenz chaos. (a) The bifurcation diagram with $X(V)$ versus V_{dc} as the control parameter. While increasing V_{dc}, a jump is observed from the S_+ steady state to the chaotic state at point A; $V_{dc}=-1.5$ V (approximately). When we decrease V_{dc} from such a high value, the chaotic state persists up to the point B; $V_{dc}=-2.5$ V (approximately). (b) Chaotic time series at $V_{dc}=-2.1$ V. Under periodic voltage ($V_{dc}=-2.1$ V, $\delta=0.014$, $\nu=1.3$ kHz), the chaotic attractor is destroyed due to a collision with the U_+ UPO, and the system goes to the controlled S_+ steady state. (d) The uncontrolled Lorenz chaos and the controlled S_+ steady state. The parameter values are the same as in (c). (e) The crisis threshold curve in V_{dc} versus δ space; $\nu=1.3$ kHz. (f) The crisis threshold curve in ν versus δ space; $V_{dc}=-2.1$ V. This curve exhibits two crisis resonance regions, one around $\nu_c=1.3$ kHz and the other around $\nu=2\nu_c$.

Fig. 1(a). We fix the value of $V_{dc}=-2.1$ V and show the chaotic time series in plot (b). Next we apply control modulation of frequency $\nu=1.3$ kHz and modulation depth δ. As we increase $\delta>0.014$, the chaotic attractor no longer remains stable. Plot (c) shows the temporal transition from the chaotic state to the controlled steady state S_+. The crisis occurs due to the collision with the UPO U_+. Plot (d) shows the uncontrolled chaotic attractor and the controlled steady state. We determine the crisis threshold amplitude at various values of V_{dc} along the multistable regime. The modulation frequency is kept constant at 1.3 kHz. Plot (e) shows the crisis threshold curve in δ versus V_{ac} space. Very similar to the theoretical results [shown in Fig. 1(e)], the threshold is maximum near the subcritical Hopf bifurcation point and decreases along with V_{dc}. Crisis threshold δ is minimum near the uncontrolled crisis condition ($V_{dc}\sim-2.5$ V). Plot (f) shows the crisis threshold curves in the modulation depth versus the modulation frequency space at $V_{ac}=-2.1$ V. We find the crisis threshold curve exhibits minimal destruction amplitude at $\nu=1.3$ kHz and at 2.6 kHz. Thus the crisis resonance frequency is 1.3 kHz. Therefore the experiments also demonstrate controlled destruction of chaos by small-amplitude parameter modulation and the existence of two crisis resonance regions in the control modulation parameter space.

Notably, after Haken's famous revelations [24] of striking similarity between the two-level laser model and Lorenz equations, extensive experiments and theory have observed Lorenz-Haken chaos and subcritical Hopf bifurcation in FIR lasers [10,11]. Therefore, we believe our concept of controlling multistability in autonomous systems is at least applicable in thermal hydraulics and FIR lasers. Moreover, since subcritical Hopf bifurcation is a generic phenomenon and the concept is based on periodic modulation of system parameters, we believe this technique should have much wider applicability. We have indeed successfully demonstrated theoretically similar destruction of chaos in the case of an optically injected multistable semiconductor laser [25]. Details of these analyses would be published elsewhere.

We may remark that the Lorenz model is a paradigm for the thermal fluid dynamics based systems where the parameters r and σ refer to Rayleigh number and Prandtl number, respectively. In actual fluid dynamical systems, the coexistence of regular (unidirectional flow with mild fluctuations of velocity) and chaotic instability (bidirectional turbulent flow with large fluctuations) states cannot be ruled out, as evident from the recent experiments with a double-channel natural convection test facility [12]. This paper reports (i) sudden jump from steady flow to the oscillatory flow at a critical condition and (ii) hysteresis between steady single-phase flow and bidirectional oscillatory two-phase flow. We believe these features are signatures of subcritical Hopf bifurcation. The bidirectional oscillatory flow could be undesirable in many applications, for instance, in the natural circulation coolant flow in the new generation natural circulation nuclear reactors [12,13,26] based electric power generators, and therefore needs attention. Conventionally, the operating regime is limited to avoid the multistable regime. However, inside the multistable regime, the operating power is higher and could be useful for handling large capacity power generation. While there may be other provisions to control mild deviations from the designed state, we believe, tackling the chaotic state is a more complex problem. In such circumstances, the small-amplitude modulation of some suitable parameters could be a very useful provision to destroy the chaotic state and as a consequence, the system comes back to the designed state.[2] Therefore, chaos-related problems may be resolved and an extension of the operating regime within the multistable region looks feasible.

[2]In the case of symmetric systems, such as Lorenz equations, there are two steady states. In fluid dynamics applications one may also correlate the same with two counterpropagating flows [12]. If the system is designed for one steady state (the flow in a preferen-

In general, a large class of nonlinear systems may be broadly classified into two categories: (i) autonomous and (ii) periodically forced (or parametrically excited). In the current paper, we have considered some standard models of autonomous systems and demonstrated the controlled destruction of chaos by small-amplitude periodic modulation of any system parameters. Multistability appears in these systems due to subcritical Hopf bifurcation. Now let us draw attention to recent reports in the case of periodically forced (parametrically excited) systems and equivalent multiparameter, multidimensional diffeomorphisms. Indeed, the periodic modulation of system parameters has been successfully applied [27] to destroy an exceedingly complex (but organized) multistable scenario, namely, the self-similar organization of Gavrilov-Silnikov-Newhouse sinks [28] in the case of the Henon map. The modulation approach has also been experimentally tested with a CO_2 laser [29] and a doped fiber laser [30]. In these experiments, laser parameters are driven by two periodic signals. The first periodic modulation makes the laser multistable where the coexisting periodic states are created by saddlenode bifurcations due to the overlap of some or other subharmonic resonances. The second modulation is then applied to destroy some of these stable periodic states suitably. Besides, a slow periodic modulation over the control parameter may induce an interaction between stable and unstable periodic orbits,[3] causing a resonance at the modulation frequency. This has been observed numerically with laser rate equations and quadratic maps, and experimentally with a cavity-loss modulated CO_2 laser [32]. Thus we believe the periodic modulation of system parameters could play a very significant role in determining the multistable nature in autonomous as well as periodically forced nonlinear systems.

To conclude, we have demonstrated that small-amplitude periodic modulation of any system parameters may lead to global changes in the dynamics of the multistable systems that exhibit simultaneous coexistence in the phase space of chaotic and steady states. In particular, such a modulation may lead to the boundary crisis of the chaotic attractor due to a collision with an UPO, and subsequent transition to the steady states. The threshold modulation depth for crisis would be minimum if the modulation frequency is equal to (or multiples of) crisis resonance frequency that is close to UPO rotation frequency. The parameter modulation concept works in the presence of noise as well. These results are theoretically demonstrated with Lorenz's equations and are in excellent agreement with experimental observations with an analog circuit of Lorenz equations.

ACKNOWLEDGMENTS

B.K.G. is sincerely thankful to E. Doedel and his associate researchers for giving free access to the AUTO software [33]. This software has been highly useful for some in-depth investigations of Lorenz equations, in particular, computing the bifurcation diagram in Fig. 1(a), UPOs, ν_s, ν_e, and ν_u. He has been helped by S. Bruggioni and F. Salvadori (from INOA, Florence, Italy) in conducting the experiments with the analog circuit. He is thankful to F. T. Arecchi, Physics Department, University of Florence, Florence, Italy for his kind suggestions and to R. Meucci, INOA, Florence for an invitation to visit INOA. He also sincerely acknowledges financial support from ICTP, Trieste, Italy via TRIL program for his visit to INOA during 2006.

tial direction), a suitable mechanism has to be kept under provision in addition to the control mechanism for destroying chaos.

[3]Nonlinear systems under periodic forcing may settle at any stable periodic (say of period n) attractor with its basin divided into n domains or segments that are in general not in phase. A chaotic or an almost periodic signal may induce coherence among those domains and make the enitre basin in-phase without any major change in the original scenario. The underlying mechanism is attributed to some sort of stochastically driven crisis. This has been demonstrated with a Duffing system having a piecewise linear circuit element in place of the conventional cubic nonlinearity [31].

[1] E. Ott, C. Grebogi, and J. A. Yorke, Phys. Rev. Lett. **64**, 1196 (1990).
[2] E. R. Hunt, Phys. Rev. Lett. **67**, 1953 (1991).
[3] T. L. Carroll, I. Triandaf, I. Schwartz, and L. Pecora, Phys. Rev. A **46**, 6189 (1992); Z. Gills, C. Iwata, R. Roy, I. B. Schwartz, and I. Triandaf, Phys. Rev. Lett. **69**, 3169 (1992); I. Triandaf and I. B. Schwartz, Phys. Rev. E **48**, 718 (1993).
[4] S. Boccaletti, C. Grebogi, Y.-C. Lai, H. Mancini, and D. Maza, Phys. Rep. **329**, 103 (2000).
[5] R. Holzner, B. Derighetti, M. Ravani, and E. Brun, Phys. Rev. A **36**, 1280 (1987); A. Baugher, P. Hammack, and J. Lin, *ibid.* **39**, 1549 (1989).
[6] J. L. Boulnois, A. Van Lerberghe, P. Cottin, F. T. Arecchi, and G. P. Puccioni, Opt. Commun. **58**, 124 (1986).
[7] Peng-ye Wang, A. Lapucci, R. Meucci, and F. T. Arecchi, Opt. Commun. **80**, 42 (1990).
[8] A. Hohl, H. J. C. van der Linden, R. Roy, G. Goldsztein, F. Broner, and S. H. Strogatz, Phys. Rev. Lett. **74**, 2220 (1996); A. Gavrielides, V. Kovanis, P. M. Varangis, T. Erneux, and G. Lythe, Quantum Semiclassic. Opt. **9**, 785 (1997); S. K. Hwang and J. M. Liu, Opt. Commun. **183**, 167 (1999).
[9] S. Wieczorek, T. B. Simpson, B. Krauskopf, and D. Lenstra, Phys. Rev. E **65**, 045207(R) (2002).
[10] C. O. Weiss and W. Klische, Opt. Commun. **51**, 47 (1984); U. Hübner, N. B. Abraham, and C. O. Weiss, Phys. Rev. A **40**, 6354 (1985); C. O. Weiss and J. Brock, Phys. Rev. Lett. **57**, 2804 (1986); C. O. Weiss, N. B. Abraham, and U. Hübner, *ibid.* **61**, 1587 (1988).
[11] R. G. Harrison, W. Lu, and P. K. Gupta, Phys. Rev. Lett. **63**, 1372 (1989); W. Lu and R. G. Harrison, Phys. Rev. A **43**, 6358 (1991).
[12] W. L. Chen, S. B. Wang, S. S. Twu, C. R. Chung, and Chin Pan, Int. J. Multiphase Flow **27**, 171 (2001); J. D. Lee and Chin Pan, Nucl. Eng. Des. **235**, 2358 (2005).

[13] Rizwan-uddin, Nucl. Eng. Des. **236**, 267 (2006).
[14] F. Ravelet, L. Marie, A. Chiffaudel, and F. Daviaud, Phys. Rev. Lett. **93**, 164501 (2004).
[15] F. T. Arecchi and F. Lisi, Phys. Rev. Lett. **49**, 94 (1982); M. R. Beasley, D. D'Humieres, and B. A. Huberman, *ibid.* **50**, 1328 (1983).
[16] G. P. King and S. T. Gaito, Phys. Rev. A **46**, 3092 (1986); **46**, 3300 (1986).
[17] Hongyan Sun, Lianxi Ma, and L. Wang, Phys. Rev. E **51**, 3475 (1995).
[18] E. N. Lorenz, J. Atmos. Sci. **20**, 130 (1963).
[19] A. Arneodo, P. Coullet, and C. Tresser, Phys. Lett. **81A**, 197 (1981); G. Demeter and L. Kramer, Phys. Rev. Lett. **83**, 4744 (1999).
[20] E. Meron and I. Procaccia, Phys. Rev. A **35**, 4008 (1987); J. M. Gambaudo, P. Glendinning, and C. Tresser, Nonlinearity **1**, 203 (1988).
[21] J. M. Lopez and F. Marques, Phys. Rev. Lett. **85**, 972 (2000).
[22] V. Carbone, G. Cipparrone, and G. Russo, Phys. Rev. E **63**, 051701 (2001); J. Abshagen, G. Pfister, and T. Mullin, Phys. Rev. Lett. **87**, 224501 (2001).
[23] R. Meucci, F. Salvadori, K. Al Naimee, S. Bruggioni, B. K. Goswami, S. Boccaletti, and F. T. Arecchi, *Conference Proceedings of the 9th Experimental Chaos Conference—ECC9, Brazil, 2006*.
[24] H. Haken, Phys. Lett. **53A**, 77 (1975); Chu-Zheng Ning and H. Haken, Phys. Rev. A **41**, 3826 (1990).
[25] S. Wieczork, B. Krasukopf, T. B. Simpson, and D. Lenstra, Phys. Rep. **416**, 1 (2005).
[26] A. Manera, U. Rohde, H.-M. Prasser, and T. H. J. J. van der Hagen, Nucl. Eng. Des. **235**, 1517 (2005); M. Furuya, F. Inada, and T. H. J. J. van der Hagen, *ibid.* **235**, 1557 (2005); **235**, 1635 (2005).
[27] B. K. Goswami and S. Basu, Phys. Rev. E **66**, 026214 (2002).
[28] B. K. Goswami, Phys. Rev. E **62**, 2068 (2000); B. K. Goswami and S. Basu, *ibid.* **65**, 036210 (2002).
[29] A. N. Pisarchik and B. K. Goswami, Phys. Rev. Lett. **84**, 1423 (2000).
[30] A. N. Pisarchik, Y. O. Barmenkov, and A. V. Kiryanov, Phys. Rev. E **68**, 066211 (2003).
[31] T. L. Carroll and L. M. Pecora, Phys. Rev. E **48**, 2426 (1993).
[32] A. N. Pisarchik and R. Corbalan, Phys. Rev. E **59**, 1669 (1999).
[33] E. J. Doedel, R. C. Paffenroth, A. R. Champneys, T. F. Fairgrieve, Y. A. Kuznetsov, B. Sandstede, and X. Wang, *AUTO 2000: Continuation and Bifurcation Software for Ordinary Differential Equations (with Homcont)*, www.ama.caltech.edu/redrod/auto2000/distribution